SOL-GEL DERIVED NANOPARTICLES AND PROCESSING ROUTES TO CERAMICS AND COMPOSITES

H. Schmidt, C. Kropf*, T. Schiestel, H. Schirra, S. Sepeur, C. Lesniak+

Institut fuer Neue Materialien
Im Stadtwald, Geb. 43 A
D-66 123 Saarbruecken
Germany

*Henkel KGaA
D-40 191 Düsseldorf
Germany

+ESK GmbH
D-87 437 Kempten
Germany

ABSTRACT

Highly crystalline nanoparticles from Y-ZrO_2 and FeO_x have been prepared by microemulsion with subsequent solvothermal treatment and by precipitation processes. In both cases, aqueous based intermediates have been prepared which have been surface-modified by carboxylic acids and aminosilane. The surface modification prevents the formation of hard agglomerates of the nanoparticles (6 - 8 nm) completely and provides complete redispersibility. Low sintering compacts and nanocomposites have been prepared, and first results for using the FeO_x nanoparticles for medical applications have been obtained.

INTRODUCTION AND GENERAL ASPECTS OF SOL-GEL NANOPROCESSING

Sol-gel processing has become a very interesting field of research since the first spectacular industrial success has been reported by Schott (Calorex®) based on the investigations of Dislich [1]. The attractiveness of sol-gel processing is based on the fact that inorganic materials can be synthesized by a chemical route having the potential to avoid high processing temperatures such as glass melting (around 1,500 °C or ceramic sintering (from 900 to over 2,000 °C). In general, the sol-gel process is carried out on the basis of soluble precursors such as metal alkoxides or silanes. These precursors are chosen very often since it is possible to obtain homogeneous solution on a molecular level, which then can be reacted to inorganic solids. Whereas in the beginning of the sol-gel technology the majority of papers was devoted to SiO_2, later on ceramic systems also became of interest [2]. Especially based on the work of Hirano [3, 4], of Chen et al. [5] and Payne [6], it could be shown that there is a very interesting potential for low temperature processing. Hirano's and Payne's investigations clearly demonstrated that sintering temperatures can be very low by preforming bonds typical for the later cera-

mic material like in barium titanates, lead titanates, PZT or lithium niobates. This also has been investigated by A. Mosset et al. [7] in the case of barium titanate.

One of the major drawbacks in sol-gel processing of ceramics is related to the low solid content of the green bodies. The low solid content of the green bodies is closely related to the gelation mechanisms. If these coatings are formed, the solid content does not play such an important role because the evaporation of solvents is relatively easy compared to large-size components. However, as pointed out by Fred Lange [8], who investigated the formation of sol-gel films, there might be a critical thickness for obtaining crack-free coatings, and in many cases, this critical thickness is considered to be ≤ 1 μm. Above this thickness, the films, in general, are not able to dissipate the stresses resulting from capillary forces of the drying sol, due to the lack of relaxation ability. This is a result of the strong interactions between inorganic macromolecules (for example silica oligomers) or colloidal particles (e.g. alumina, titania, zirconia and others), leading to highly brittle gels with very low strength. Zarzycki [9] has given experimental data about the strength of silica gel, which is discouragingly weak. In order to improve the processing of gels, several routes have been tried. There are some routes which propose to reduce the interaction of liquids and the pore walls of gels by using solvents other than water or to add components acting as surfactants [10, 11]. Other routes are to reduce the particle-to-particle interaction by surface modification as shown by Schmidt [12]. Surface modification of sol particles may lead to a substantial reduction of the interparticular interaction with the possibility of increasing the solid content of sols and the film thickness, as shown by Mennig [13].

Sols, in general, are stabilized by electric charges by Stern's potential [14]. The "thickness" of the electric charge double layer depends on many parameters, such as ionic strength of the solution, pH value, chemical surface properties of the particles. The transition of an electrostatically stabilized sol into a gel by removal of the electric charges by shifting the system to the point of zero charge or by reducing the sol particle distance below the Stern's repulsion potential, which then changes into attraction, leads to a fast agglomeration reaction, due to the high surface area and the unavoidable presence of reactive groups. This, in most cases, leads to a random distribution of the sol particles which, in general, is far away from a dense packing and, in general, not to a narrow pore size distribution. This may be different in thin films, as shown by Brinker with SAW measurements [15]. The sintering of low density broad pore size distribution gels, in general, leads to a very flat sintering curve with the necessity of using high temperatures for obtaining full density. This can be explained with the fact that areas with small pores sinter at low temperature, even enlarging the large pores, which then have to be densified by high temperatures, and no reasonable advantages are obtained, compared to conventional powder technology. This was

one of the reasons that most of the efforts to use sol-gel processing for ceramic parts fabrication have been abandoned.

Recently, nanostructured materials have gained high interest in science as well as in industry. Based on the early fundamental work of Gleiter and his interesting results in ceramics [16, 17], a high industrial potential is attributed to nanostructured inorganic materials. This is a result of the interesting properties of the nanoparticles [12], which is based on their high surface area, quantum size effects, high reactivity, electronic or magnetic size effects or nonlinear-optic effects. Various methods for the fabrication of nanoparticles are investigated. Most of them are related to evaporation condensation methods, plasma methods, laser or other physical methods. A few of them are related to chemical methods like the CVR (Chemical Vapor Reaction) process of H. C. Starck [18], flame spray or flame pyrolysis or hydrolysis processes. In addition to this, wet chemical methods also became of interest, for example, microemulsion processes [19, 20, 21, 22]. One of the drawbacks of the microemulsion techniques, however, is the presence of emulsifiers which, in connection with nanoparticles, in general, contribute substantially to the solid content and, in many cases, are in the range of 50 wt.-%. This causes problems in the processing of the particles or in forming agglomerate-free inorganic powders or in fabricating parts [23]. Other routes are based on the so-called controlled growth process [12, 24] and have shown that in selected systems (zirconia) the particle growth can be controlled by short molecules acting as surfactants [25, 26, 12, 24]. Very good results for the fabrication of agglomerate-free nanopowders have been obtained by the use of oligomers very stably bonded to the surface so that they can even survive hydrothermal treatments, and then, in order to decrease the organic content, to replace them by small molecules [27].

In this paper, several principles for the surface modification of nano-scale particles during or after production are investigated, and it is shown how these particles are able to be used for ceramic and composite materials fabrication.

EXPERIMENTAL

For the synthesis of nanocrystalline Y_2O_3/ZrO_2, microemulsions were prepared by mixing 57.2 ml cyclohexane, 28.6 ml of an aqueous solution of $ZrO(NO_3)_2$ ($C_{(Zr)}$ = 0,4 mol/l) and $Y(NO_3)_3$ ($C_{(Y)}$ = 0,03 mol/l) and 14.3 ml of oleic acid polyethyleneoxide ester ($(CH(CH_2)_7CH{=}CH(CH_2)_7CO_2[(CH_2)_2O]_{20}$, OPE) as emulsifier [20]. After stirring at 34 °C for 3 h stable, transparent microemulsions were obtained. Precipitation was carried out by bubbling NH_3 through the microemulsion until a pH value of 10 was achieved. The water was removed by azeotropic distillation, afterwards the cyclohexane was evaporated at 40 °C and 20 mbar. In order to remove excess OPE, the resulting powder was extracted with 2-propanol in a Soxhlet apparatus. The extracted, modified powder was redis-

persed in a 1 : 1 water/ethanol mixture (solid content: 10 wt. %) and the resulting suspension was hydrothermally treated (250 °C, 75 bar, 3 h). The solid was separated by centrifugation (4000 r/min, 15 min), after the pH was adjusted to pH = 5.9, the point of zero charge of the powder, and dried at 60 °C and 20 mbar.

In order to exchange the OPE bound on the particles` surface, 50 g of the powders were suspended in 200 ml of 8 N NaOH and 200 ml toluene were added and stirred for 5 h to extract hydrophobic reaction products. The mixture was heated under reflux for 5 h. After the deesterification the solid was separated from the liquid phase after the pH of the aqueous suspension was adjusted to pH = 7 (point of zero charge of ZrO_2) by centrifugation (4000 r/min, 15 min). In order to remove soluble reaction products, the resulting sediment was repeatedly diluted with 1 liter of deionized water, flocculated by pH-adjusting to pH = 7 and filtrated until the conductivity of the washing water was below 5 µS. As surface modifier 4 g of trioxadecanic acid (TODS) were added to the resulting suspension. After stirring for additional 3 h the pH of the suspension was adjusted to pH = 8 (point of zero charge of the TODS-modified ZrO_2) and the flocculated powders were washed as described above in order to remove excess TODS not bound onto the particles` surface. Finally, the powder was isolated by filtration and dried (60 °C, 20 mbar, 5 h). The synthesized powders were characterized by HRTEM, x-Ray, IR-spectroscopy, and laser backscattering. For the fabrication of ZrO_2 containing high refractive index hard coatings, 20 g of the prepared ZrO_2 powders were dispersed in 100 ml distilled water and mixed with a butanolic solution of a boehmite containing condensate with epoxysilane (hard coating basis material) as described in detail in [28, 29] up to a concentration of 30 - 40 wt.-% of ZrO_2. The clear liquid was used to coat polycarbonate lenses pretreated by a plasma in a dip coating procedure. After drying, the coating was cured at 130 °C for 2 hrs.

For the preparation of nano-scale iron oxide, 89.40 g of ferrous chloride tetrahydrate ($FeCl_2*4H_2O$) and 243,3 g of ferric chloride hexahydrate ($FeCl_3*6H_2O$) were dissolved in 2 liters of oxygene-free deionized water. 5 M NaOH was added until a pH of 11.5 is reached. The mixture was heated up to 65 °C for 10 min. The resulting black precipitate was washed repeatedly with deionized water. For surface modification, to an acidic (pH 5) aqueous suspension of iron oxide (5 wt.-%) γ-aminopropyl triethoxysilane (APS) was added until a weight ratio silane to iron oxide of 0.8 was reached. The suspension was pourred into ethyleneglycol (water/ethyleneglycol; v/v=1), heated up to 80 °C and sonified for 48 hours. Subsequently, water and ethanol were distilled off under vacuum at 50 °C. The glycolic suspension was centrifuged for 60 min at 2500 m/s², and the supernatant colloidal suspension was dialyzed against deionized water. The as prepared particles were characterized with respect to particle/agglomerate size by laser light scattering and TEM. Surface chemical

properties were determined by zeta potential measurements and their composition were analyzed by ICPAES.

RESULTS

Zirconia and Zirconia Composites

As shown elsewhere [30], microemulsion systems based on ZrO_2 and yttria-ZrO_2 have been used for the fabrication of zirconia nanoparticles. However, the removal of the emulsifiers by oxidation at elevated temperatures leads to strongly agglomerated powders. For this reason, a method has to be developed, which allows the preparation of well crystallized powders at temperatures where no agglomeration takes place. Solvothermal treatment in the presence of surface protecting components seemed to be an adequate means. A microemulsion has been prepared from zirconium and yttrium nitrates in cyclohexane by dispersing the aqueous nitrate solution in the organic solvent in the presence of OPE. OPE was chosen since it was known to be an effective emulsifier as well as to adsorb strongly to oxide surfaces. After three hours stirring, completely transparent microemulsions have been obtained. At this temperature, relatively high water-to-cyclohexane ratios could be realized, as described in [31]. The emulsifier concentration, however, is rather high and requires about 15 % by volume of the total solution, which leads to a rather high organic content in the whole system. The droplet size under these conditions is 13 nm. Precipitation within the droplets is obtained by NH_3 bubbling. After the removal of cyclohexane and water by vacuum treatment and azeotropic distillation, the particle size is in the range between 2 and 3 nm, as shown in fig. 1 from the TEM micrograph.

The X-ray analysis of these powders clearly indicates that the crystallinity of these precipitates is rather poor. Due to the poor crystallinity, a solvothermal treatment at 250 °C for three hours was carried out, and after the treatment, the separation of the powder from the solvent was performed by repeatedly washing and centrifugation, leading to NH_4NO_3-free powders. After centrifugation the FTIR spectra were taken (fig. 2). They clearly show that the OPE still is linked to the surface of the particle and the photon correlation spectroscopy for the determination of the particle size shows that the particle size has increased to about 3 - 10 nm, indicating a growth reaction in the presence of OPE (figs. 3 and 4) [31]. The powders can be redispersed in water completely agglomerate-free.

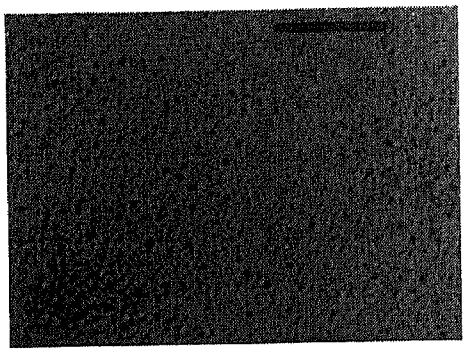

20 nm

Fig. 1: TEM micrograph of the OPE coated Y-ZrO_2 powder after the microemulsion preparation.

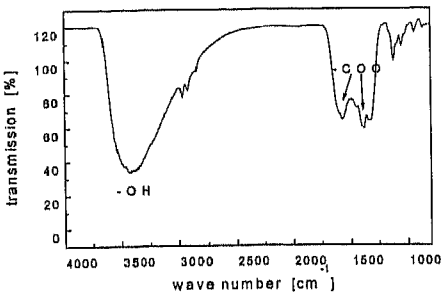

Fig. 2: IR-spectrum of Y_2O_3/ZrO_2 nanoparticles coated with OPE after precipitation from the microemulsion..

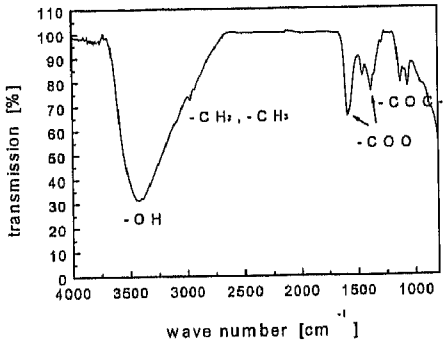

Fig. 3: IR-spectrum of the washed ZrO_2 nanoparticles coated with OPE after hydrothemal crystallization at 250 °C, 75 bar, 3 h.

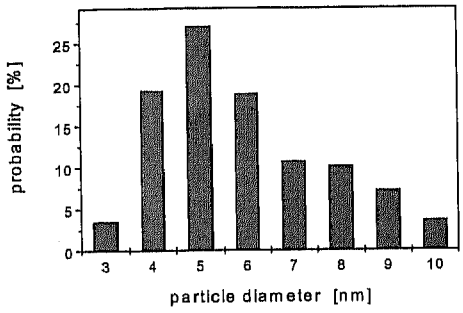

Fig. 4: Particle size distribution calculated from HRTEM micrograph of hydrothermal crystallized Y_2O_3/ZrO_2 (250 °C, 75 bar, 3 h) surface modifier coated with OPE.

In fig. 5 the HRTEM micrograph of these powders is shown, and fig. 6 shows that these powders now exhibit a good crystallinity (cubic modification), the line broadening of which matches with the observed particle size. This indicates that mass transport as well as crystallization can take place under solvothermal conditions under the surface protecting effect of OPE.

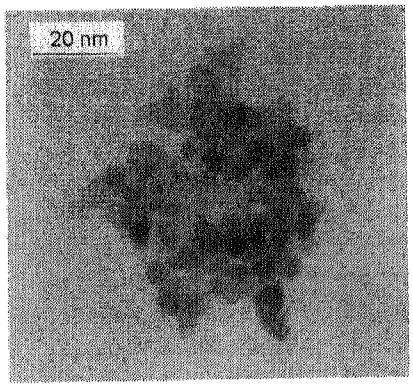

Fig. 5: HRTEM micrograph of Y_2O_3/ZrO_2 after hydrothermal crystallization (250 °C, 75 bar, 3 h), surface modifier: OPE.

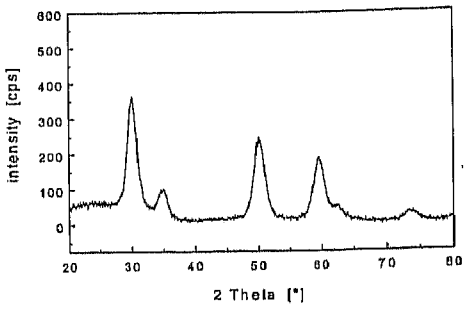

Fig. 6: X-ray diffraction spectrum of Y_2O_3/ZrO_2 after hydrothermal crystallization (250 °C, 75 bar, 3 h).

In [27] it was shown that Y-ZrO_2 powders obtained from controlled growth precipitation processes covered with polymeric protective components could be reacted with smaller molecules to reduce the organic content without losing their surface protection. For this reason, a process was employed, the experimental of which was described elsewhere [27]. The OPE-modified particles were treated with a two-phasic mixture of toluene and sodium hydroxide. The sodium hydroxide removes the OPE, which then is subsequently dissolved in the toluene phase, and at the same time, a negative ζ-potential is established on the zirconia particle surface in order to avoid aggregation. After changing the pH to 7, flocculation takes place in the system, and it can easily be separated by centrifugation from the liquid. The powder repeatedly was washed with deionized water. After washing to neutral pH, carboxylic acid (trioxadecanic acid) was added, which led to a complete redispersion of the powder, and as investigated by photon correlation spectroscopy, the particle size distribution remains unchanged compared to the state after the hydrothermal treatment. These powders are completely redispersible in water as well as in ethanol, and it could be shown by DRIFT spectroscopy that the carboxylic acid is bonded to the particle surface (fig. 7), since the position of the =C=O peak represents the carboxylate ion. The process shows that the flocculated system is only weakly agglomerated and can be recoated by carboxylic acids before hard agglomerates are formed. The total organic content now is reduced to < 5 wt.-%, representing an almost 75 % coverage of the nanoparticle surface. As also shown in [27], the ζ-potential is shifted to positive values.

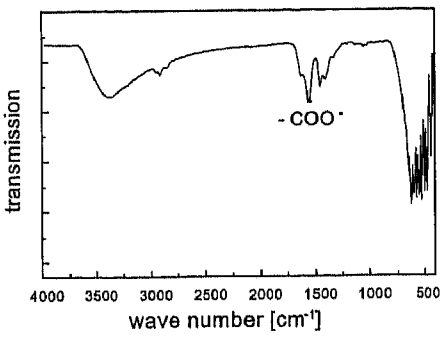

Fig. 7: IR-spectrum of the TODS-modified Y_2O_3/ZrO_2.

Compacts prepared from these powders by cold isostatic pressing can be sintered to full density at 1130 °C, as shown in fig. 8. The pores of the green bodies made from these powders measured by BET show a narrow size distribution with a maximat 3.5 nm, which is in a good agreement with the values calculated from the particle size distribution. The sintering curve of the green body (fig. 8b) shows a one step sintering behavior which was finished at a temperature of 1100 °C.

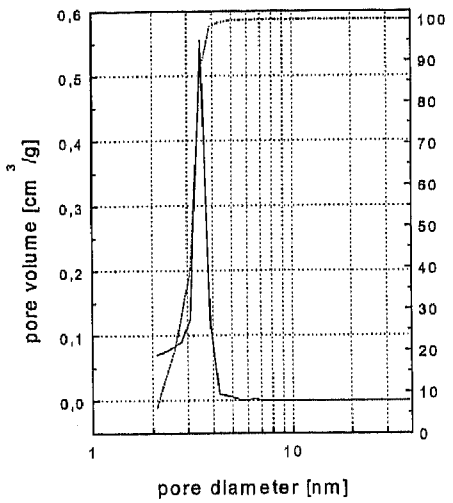

Fig. 8a: Pore size distribution of cold pressed hydrothermally crystallized Y_2O_3/ZrO_2 powder.

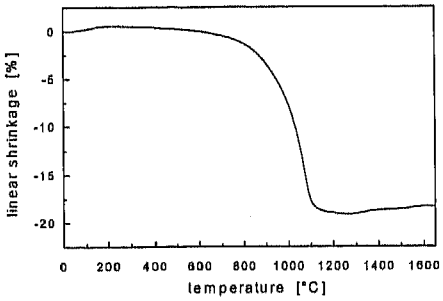

Fig. 8b: Sintering curve of cold pressed hydrothermally crystallized Y_2O_3/ZrO_2 powder (96 % density).

The low sintering temperature obtained from cold pressing which is, in general, not the most favorable way to produce green bodies from nanopowders, is attributed to the effect of ODS as pressing aid leading to a monomodal nanoporosity. The yield of the microemulsion/solvothermal process sums up to 3.4 g powder per 100 ml of reaction volume. Due to the solvothermal treatment, no high temperature calcination step is necessary to obtain highly crystalline powders. The obtained results show that OPE can be used as an emulsifier and, at the same time, as protecting agent during the hydrothermal process. Through the washing steps, all soluble salts such as nitrates can be removed completely. Depending on the type of processing, solid contents of green compacts up to 50 % by volume could be fabricated. The highest green densities could be obtained by a compounding process with subsequent extrusion [32].

For the fabrication of transparent hard coatings, these powders were suspended in water and formed a clear solution. This solution was mixed with a hard coating system described in [28]. Coatings on polycarbonate eye glass lenses have been fabricated by dip coating of the plasma pretreated lenses. Plasma treatment leads to a good adhesion on the substrates surface with cross-cut/tape test according to DIN 53151-A-B and 58196-K2 show values of CC/TT = 0-1/0-1. The abrasion resistance of the zircon dioxide-modified hard coatings (film thickness: 3 - 5 μm) was determined by the Taber Abraser test according to DIN 52347 (1,000 cycles/abrasion wheels: CS-10F/5,4 N). The wear resistance of a system containing 30 % zircon dioxide is down to ≈ 5 % haze after 1,000 cycles. The refractive index is close to 1.6.

In order to fabricate iron oxides, which basically can also be carried out by micro-emulsion techniques [33]), a more simple route was investigated. There is a large body of literature [34, 35, 36, 37, 38] available which shows that iron oxide nanoparticles can be easily precipitated from aqueous solutions. However, the problem of agglomeration is still difficult according to the state of the art. Since it can be assumed that in the presence of water the agglomeration of iron oxide particles is weak, a step was anticipated to deagglomerate the iron oxide in presence of surface modifiers. In fig. 9 and fig. 10 the particles and the particle size distribution of iron oxide as precipitated is shown. The primary particle size ranges from 8 - 12 nm, however, the particle size obtained from laser back scattering ranges from 30 - 100 nm which is due to agglomerates still stable under measuring conditions.

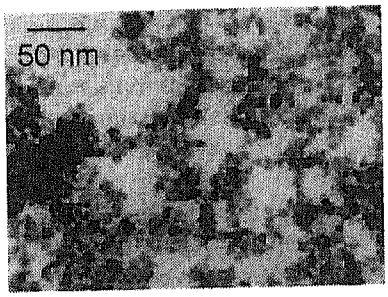

a

Fig. 9: TEM micrograph of unmodified iron oxide particles.

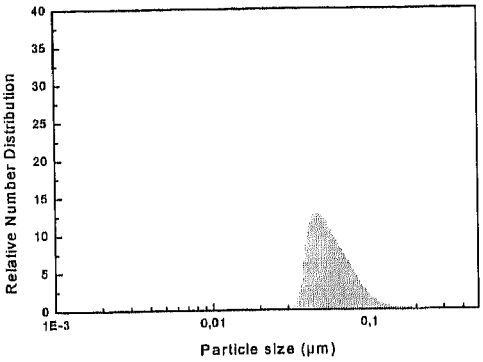

b

Fig. 10: Particle size distribution of iron oxide in aqueous suspension (determined by laser light scattering).

According to x-ray analysis (fig. 11), the particles consist of either magnetite or maghemite. Both nanocrystalline phases cannot be distinguished due to the almost identical lattice parameters. From the peak broadening, a crystallite size of 9 nm was calculated using the Scherrer equation. Due to the small particle size, superparamagnetic behaviour is expected. Measurements in a vibrating sample magnetometer revealed a saturation magnetization of 68 EMU/g (bulk magnetite 122 EMU/g, bulk maghemite 108 EMU/g). The absence of a hysterisis loop indicates superparamagnetic properties (fig 12). For deagglomeration and stabilization of the FeO_x particles, the treatment of the slurry with γ-aminopropyl triethoxysilane was carried out as described in the experimental.

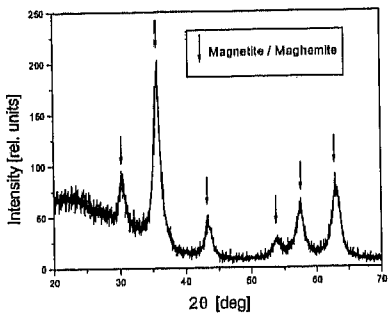

c

Fig. 11: X-ray diffraction diagramm of iron oxide powder.

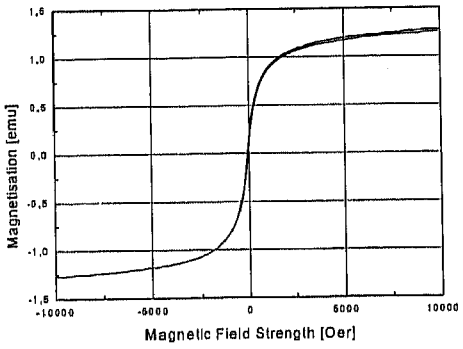

d

Fig. 12: Magnetization curve for unmodified iron oxide particles.

In fig. 13 the particle size distribution determined with laser backscattering is shown before and after surface modification. The average particle size is shifted from 50 nm to 10 nm. Compared with the primary particles size derived from TEM micrograph (see fig. 9) it can be concluded that the particles are completely deagglomerated. In additon no agglomerates can be found on TEM micrographs after surface modification (fig. 14).

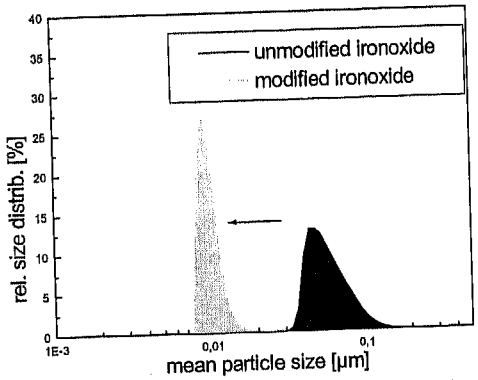

Fig. 13: Comparison of particle size distribution for unmodified and modified iron oxide (measured by laser light scattering).

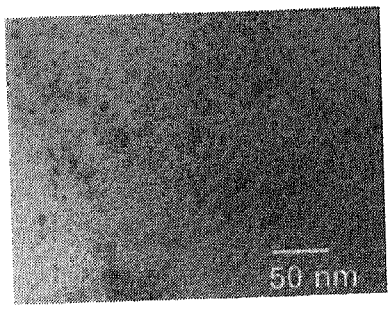

Fig. 14: TEM micrograph of a silane modified iron oxide.

To demonstrate the effect of surface modification on the surface chemical properties, ζ-potential measurements of unmodified and modified iron oxide were compared (fig. 15). After the modification, the particles possess an isoelectric point of 9.5 (unmodified particles IEP of 6), indicating the presence of free amino groups on the particle surface. A silane content between 4 and 5 rel. wt.-% was determined by chemical analysis. From this value a monomolecular layer around the iron oxide particle can be calculated (average molecule size aminosilane appr. 60 A^2). Fig. 16 shows a structure model for the prepared particles. Aqueous suspensions of functionalized iron oxide are stable against agglomeration for a long time (> 6 months) and a desorption of the coating was not observed.

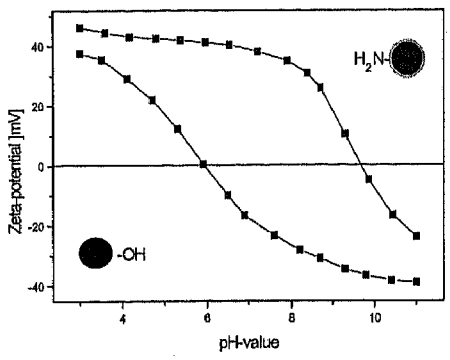

Fig. 15: Zetapotential vs. pH curves for unmodified and modified iron oxide.

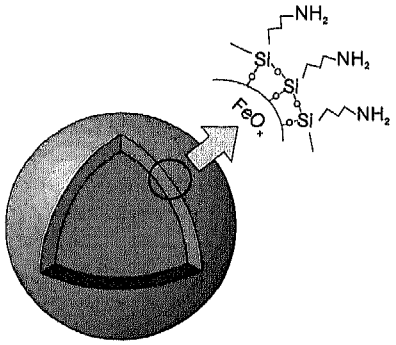

Fig. 16: Core-shell structure model for the functionalized particles.

Medical Applications

The superparamagnetic iron oxide nanoparticles described above possess interesting properties for medical applications. Their size in combination with suitable surface chemical properties makes a recognition by reticuloendothelial system difficult. This allows an application as drug carrier systems. Their magnetic properties can be used for a new hyperthermic cancer therapy, which is based on the following principles:

Superparamagnetic particles get magnetized in a magnetic field. If the field is switched off the particles dissipate their magnetic energy into thermal energy. If these particles are brought into tumor tissue a controlled heating is possible by applying an external AC magnetic field. This therapy is called "magnetic fluid hyperthermia".

In in-vitro experiments aminosilane modified iron oxide nanoparticles the details of which are described elsewhere [39, 40] showed a higher uptake into malignant cells (fig. 17) compared to normal cells. The tumor cells eagerly consume these nanoparticles but are not able to digest them. Irradiation by an alternating magnetic field led to heating up of the cells and their destruction.

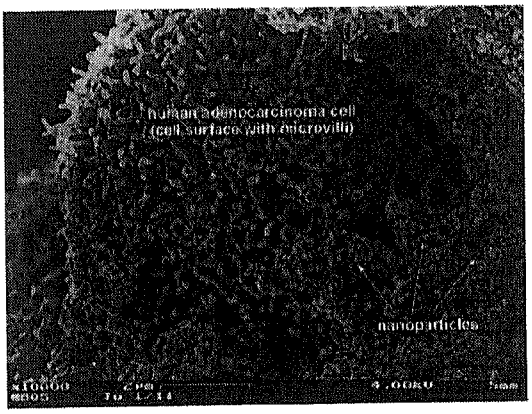

Fig. 17: REM picture of a malignant cell in the presence of aminosilane modified iron oxide particles.

CONCLUSIONS

The experiments show that sol-gel preparation techniques carried out under "protective" conditions can be used to prepare agglomerate-free nanoparticles with specific surface functions. Using this approach, nanoparticles can be used advantageously for ceramic parts processing, for polymer matrix nanocomposite hard coating fabrication and for medical application.

ACKNOWLEDGEMENT

The authors want to thank Mr. D. Burgard and Mr. N. Bendzko for their helpful discussions, the European Commission Directorate-General XII, the Ministry for Research and Culture of Saarland and the Federal Ministry for Research and Technology for their financial help.

REFERENCES

[1]H. Dislich, Angew. Chem. 83, p. 428 (1971).

[2]C. J. Brinker, and G. W. Scherer, Sol-Gel Science, Academic Press, London, 1990.

[3]S. Ono and S.-I. Hirano, "Synthesis of Highly Oriented Lithium Niobate Thin Film from Neutralized Aqueous Precursor Solution", *J. Am. Ceram. Soc.*, **80** [11] 2869-2875 (1997).

[4]S.-I. Hirano and K. Kato, "*Manufacture of Lithium Niobate Powder*", Japanese Patent No. JP 01 09 34 25 A2, April 12, 1989.

[5]E. Wu, K.C. Chen, J.D. Mackenzie, „Ferroelectric Ceramics - The Sol-Gel Method versus Conventional Processing", *Mat. Res. Soc. Symp. Proc.* **32**, 169 (1984).

[6]D.A. Payne, p. 39 in *Proceedings International Symposium on Molecular Level Designing of Ceramics*, Nagoya, March 1991. Edited by Team on the NEDO International Joint Research Project, 1991.

[7]A. Mosset, I. Gautier-Luneau, J. Galy, P. Strehlow and H. Schmidt, "Sol-Gel Processed $BaTiO_3$ - Structural Evolution from the Gel to the Crystalline Powder", *J. Non-Cryst. Solids* **100**, 339 - 344 (1988).

[8]F.F. Lange, "Processing-Related Fracture Origins: I, Observations in Sintered and Isostatically Hot-Pressed Al_2O_3/ZrO_2 Composites", *J. Am. Ceram. Soc.* **66**, 396-398 (1993)

[9]J. Zarzycki, Synthesis of Glasses from Precursor: Bulk and Film - a Comparison, *Proc. of the European Meeting Inorganic Coatings on Glass.* Edited by P. Picozzi, S. Santucci, P. Boattini, L. Massarelli and V. Scopa, Soietà Italiana Vetro, L'Aquila, Italy, 149 (1988).

[10]R.K. Iler, „The Chemistry of Silica". J. Wiley & Sons, New York, 1979.

[11]S. Wallace and L.L. Hench, "The Processing and Characterization of CDDA Modified Gel-Derived Silica", in: *Better Ceramics Through Chemistry.* Edited by C.J. Brinker, D.E. Clark, D.R. Ulrich. North-Holland, New York, 19984.

[12]H. Schmidt, KONA Powder and Particle, No. **14**, 92 - 103 (1996).

[13]M. Mennig, G. Jonschker and H. Schmidt, "Sol-Gel Derived Thick SiO_2 Coatings and Their Thermomechanical and Optical Properties, *SPIE Proc. Sol-Gel Optics* **1758**, 125 - 134 (1992).

[14]O. Stern, *Z. Elektrochem.*, **508** (1924).

[15]G.C. Frye, A.J. Ricco, S.J. Martin and C.J. Brinker, "Characterization of the Surface Area and Porosity of Sol-Gel Films Using SAW Devices", pp. 349 - 354 in *Better Ceramics Through Chemistry.* Edited by C.J. Brinker, D.E. Clark and D.R.Ulrich, Materials Research Society, Pittsburgh, PA, 1988.

[16]H. Gleiter, Nanocrystalline Materials, Pergamon Press, Oxford, 1989.

[17]H. Gleiter, R. Birringer and J. Karch, "Verfahren zum Herstellen eines plastisch verformbaren keramischen oder pulvermetallurgischen Werkstoffes und unter Anwendung eines solchen Verfahrens hergestellter Gegenstand", European Patent No. 0 317 945 B1, Nov. 22, 1988.

[18]R. L. Meisel, T. König, in: Werkstoffwoche 1996, Symp. 9 Neue Werkstoffkonzepte, edited by H. Schmidt and R. F. Singer, (DGM Informationsgesellschaft mbH, Frankfurt/M., 1997).

[19]K. Osseo-Asare and F. J. Arriagada, Ceramic Transactions 12, Ceramic Powder Science III, edited by G. L. Messing, S. Hirano and H. Hausner, (American Ceramic Society, Westerville / Ohio, USA, 1990) 3-16.

[20]S. D. Ramamurthi, Z. Xu und D. A. Payne, *J. Am. Ceram. Soc.* **73**, 2760-63 (1990).

[21]R. Naß, D. Burgard, H. Schmidt, in: "Proceedings of the 2nd European conference on Sol-Gel Technology", edited by R. Naß, H. Schmidt and S. Vilminot, North Holland Publishers, Amsterdam, The Netherlands (1992).

[22]D. Burgard, Master Thesis, University of Saarbrücken, Germany 1992.

[23]H. Herrig. R. Hempelmann, *Mater. Lett.*, **27** [6], (1996), 287-292.

[24]D. Burgard, R. Naß and H. Schmidt, Synthesis and colloidal processing of nanocrystalline (Y_2O_3 stabilized) ZrO_2 powders by a surface free energy controlled process, in *Mat. Res. Soc., Symp. Proc.*, Pittsburgh/PA, 432:113 (1997).

[25]E. Scolan, J. Maquet, C. Bonhomme, F. Ribot and C. Sanchez, "Synthesis-Characterization-Reactivity of Titanium Oxo Nano-Building Blocks: from Oxo-Alkoxo Titanium Clusters to TiO_2 Nanoparticles", Proc. MRS Spring Meetings, April 13 - 17, 1998, San Francisco (in print).

[26]R. Naß and H. Schmidt, Formation and properties of chelated alumium-alkoxides, in: *Ceramic Powder Processing Sciencs.* Edited by H. Hausner, G. L. Messing and S. Hirano, Deutsche Keramische Gesellschaft e. V., Köln, 69 - 76 (1989).

[27]H. Schmidt, R. Nass, D. Burgard and R. Nonninger, "Fabrication of Agglomerate-Free Nanopowders by Hydrothermal Chemical Processing", Proc. MRS Spring Meeting, April 13 - 17, 1998, San Francisco (in print).

[28]R. Kasemann, H. Schmidt and E. Wintrich, "New Type of a Sol-Gel-Derived Inorganic-Organic Nanocomposite", in *Mat. Res. Soc. Symp. Proc.* **346**, 915 - 921 (1994).

[29]H. Schmidt, E. Arpac, H. Schirra, S. Sepeur and G. Jonschker, "Aqueous Sol-Gel Derived Nanocomposite Coating Materials", Proc. MRS Spring Meeting, April 13 - 17, 1998, San Francisco (in print).

[30]D. Burgard, Master's Thesis, University of Saarland, Saarbruecken, Germany (1991).

[31]C. Kropf, Ph. D. Thesis, University of Saarland, Saarbruecken, Germany (1998).

[32]to be published later.

[33]to be published later.

[34]R. Massart, "Preparation of Aqueous Magnetic Liquids in Alkaline and Acidic Media", *IEEE Trans. Magn.* **17**[2], 1247-1248 (1981).

[35]H. Pilgrimm, "Stabile magnetische Flüssigkeitszusammensetzungen und Verfahren zu ihrer Herstellung und ihre Verwendung", German Patent DE 3709852, 1984.

[36]R.E. Rosensweig, "Ferrohydrodynamics", Cambridge University Press, Cambridge, 1985.

[37]T. Sato, T. Iijima, M. Seki, N. Inagaki, „Magnetic Properties of Ultrafine Ferrite Particles", *J. Magn. Magn. Mat.* **65,** 252-256 (1987).

[38]N.M. Gribanov, E.E. Bibik, O.V. Buzunov, V.N. Naumov, "Physico-Chemical Regularities of Containing Highly Dispersed Magnetite by the Method of Chemical Condensation", *J. Magn. Magn. Mat.* **85,** 7-10 (1990).

[39]A. Jordan, P. Wust, R. Scholz, H. Faehling, J. Krause, R. Felix, "Magnetic Fluid Hyperthermia", in: *Scientific and Clinical Applications of Magnetic Carriers.* Edited by Häfeli et al., Plenum Press, New York, 1997, 569 - 595.

[40]A. Jordan, R. Scholz, P. Wust, H. Faehling, J. Krause, W. Wlodarczyk, B. Sander, T. Vogl, R. Felix, "Effects of Magnetic Fluid Hyperthermia (MFH) on C3H Mammary Carcinoma *in vivo*", *Int. J. Hyperthermia*, Vol. **13**, [6], 587 - 605 (1997).